Carbon-13 Shift Tensors in Polycyclic Aromatic Compounds. 8.[1] A Low-Temperature NMR Study of Coronene and Corannulene

Anita M. Orendt, Julio C. Facelli,[†] Shi Bai, Amarjit Rai,[‡] Michele Gossett,[§] Lawrence T. Scott,[‡] Juliana Boerio-Goates,[§] Ronald J. Pugmire, and David M. Grant*

Departments of Chemistry and Chemical and Fuels Engineering, and Center for High Performance Computing, University of Utah, Salt Lake City, Utah 84112; Department of Chemistry, Boston College, Chestnut Hill, Massachusetts 02467; and Department of Chemistry, Brigham Young University, Provo, Utah 84602

Received: August 26, 1999; In Final Form: October 15, 1999

The principal values of the ^{13}C chemical shift tensors were measured for coronene and corannulene, both at room temperature and at approximately 100 K. At room temperature the molecules are moving, resulting in a motionally averaged powder pattern. A comparison of the principal values between the room temperature motionally averaged pattern and the low-temperature static pattern provides experimental information about the orientation of the principal axis system of the shift tensor for the bridgehead carbons in these molecules. For corannulene, the orientation of δ_{33} component was determined to lie at an angle of 13° from the rotation axis (the 5-fold symmetry axis of the molecule) for the inner bridgehead carbons and at an angle 26° from this same rotation axis for the outer bridgehead carbons. These orientations are in good agreement with the angles necessary to place the δ_{33} component along the p orbitals involved in π-bonding at these carbons. In the case of coronene, the differences between the principal values at the two temperatures indicate there is an angle of 14° between the axis of rotation and the δ_{33} component for both the inner and outer bridgehead carbons. This indicates that the motion is not constrained to simple in-plane rotation, but must also have an out-of-plane component. Quantum chemical calculations of the shielding tensors were also completed using both experimental and optimized molecular geometries. The results of the calculations are in good agreement with the experimental findings.

Introduction

Over the past decade there has been increased interest in the measurement of the ^{13}C chemical shift tensors of condensed aromatic hydrocarbons, especially in the unsubstituted parent compounds. This work has provided insight into the electronic structure of the aromatic π-system and correlations have been found between the shift tensor and structural deformations in these rigid ring systems. The NMR tensor data is often difficult to obtain, mainly due to the complexity of the samples and the long relaxation times. Furthermore, the isotropic chemical shifts typically fall in a very narrow range of about 120−140 ppm, leading to a high degree of overlap for the powder patterns of the various inequivalent carbons. For these reasons, single-crystal NMR techniques,[2,3] with their very narrow lines, have been widely used in this class of compounds. The chemical shift tensors have been measured from single crystals of fluorene,[4] pyrene,[5] naphthalene,[6] acenaphthene,[7] perylene,[8] and triphenylene.[1] There are cases, however, where single crystals of sufficient size for the NMR experiment cannot be grown. In these cases one has to rely on powder NMR techniques to obtain the principal values of the shift tensor. In this paper, powder techniques are used to obtain the NMR data on two large polycyclic aromatic hydrocarbons: coronene and corannulene. The structures of both molecules are shown in Figure 1, along with that of circumcoronene.

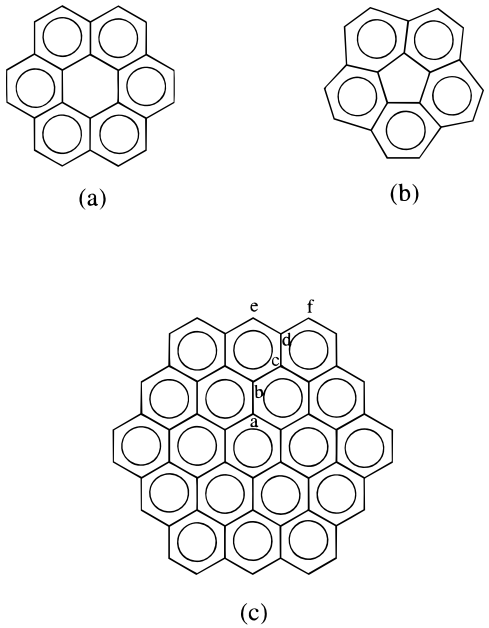

Figure 1. Structure of (a) coronene, (b) corannulene, and (c) circumcoronene.

Coronene is considered to be a model system for graphite, one of the allotropes of elemental carbon. While there have been several reports of the principal values of the chemical shift tensor in graphite,[9] the reported values vary considerably. This may be attributed to the difficulty in obtaining a high-quality spectrum, as the spectrum is broadened and has poor signal to noise due to the presence of free electrons in the sample. Coronene is the smallest molecule that possesses the local

[†] Center for High Performance Computing, University of Utah.
[‡] Boston College.
[§] Brigham Young University.

10.1021/jp993057k CCC: $19.00
Published on Web 12/09/1999

sixfold symmetry of graphite. Two previous ^{13}C NMR principal value measurements have been published on this molecule.[10,11] The first study[10] reported 1D CP spectra taken at a number of different contact times at both room temperature and at 132 K on a sample that was irradiated with ^{60}Co γ-rays in order to decrease the proton relaxation times. The 132 K spectra were only sufficient to extract two approximate tensors: an axially symmetric tensor that was attributed to the inner bridgehead carbons and a second tensor that was attributed to both the outer bridgehead carbons as well as the protonated carbons. The corresponding room temperature spectra exhibited three axially symmetric tensors, and a tentative pairing between the three parallel and perpendicular components was presented. The second literature report[11] on coronene is a 2D chemical shift−chemical shift correlation experiment at room temperature which unequivocally provides the pairing of the three parallel components with the corresponding three perpendicular components. Both the principal values and the assignment of components agree between the two room temperature literature reports. In addition, an earlier ^1H second moment study[12] at 132 K indicates that the in-plane rotational motion of the coronene molecule is slow enough on the NMR time scale (^{13}C frequency of 50 MHz) to allow for the measurement of the static or unaveraged tensors at this temperature.

Corannulene, dibenzo[*ghi*,*mno*]fluoranthene, is of special interest due its nonplanarity, and because it comprises a moiety of the fullerene C_{60} molecule. The ^{13}C resonances of carbons in five-membered aromatic rings generally have distinctive isotropic chemical shift values of 140−150 ppm. Such downfield isotropic chemical shifts have also been observed in heterogeneous materials such as soot and high-rank coals, leading researchers to suggest that five-membered aromatic ring structures may be an important component of these materials. Unfortunately, for the reasons outlined earlier, there have been only two measurements of the principal values of the shift tensor in polycyclic aromatic hydrocarbons with five-membered rings. The data are limited to measurements on fluorene[4,13] at room temperature and on C_{60}[14] at both room and low temperature. Corannulene is spinning rapidly about its fivefold symmetry axis at room temperature in the solid state, requiring the use of low temperature to eliminate the rotational motion that averages the principal values of the chemical shift tensors.

A comparison of the motionally averaged and static principal values, along with a model for the motion, can provide information about the orientation of the principal values in the molecular frame,[15] and hence details on structural deformations from planarity. This type of analysis has been completed on ferrocene[16] and permethylferrocene.[17] While the analysis can provide the angle between the axis of rotation and one of the components, the experiment does not determine the sign of the directional cosine of this angle. Hence, theoretical calculations of the shielding tensor are used to provide additional information on the angle between the rotation axis and the chemical shift tensor components.

Experimental Details

Samples. The coronene was obtained from Aldrich Chemical Co. and used without further purification. Corannulene was prepared according to the recently published three-step synthesis.[18]

NMR Measurements. All NMR measurements were made on a Varian VXR-200 spectrometer. CP/MAS spectra were obtained using a high-speed MAS probe from Doty Scientific. Static measurements were made using a large-volume (1.5 cm^3) home-built probe[19] optimized for the magic angle turning (MAT) experiment.[20] A number of experiments were performed on each sample. At room temperature, a 2D MAT experiment was acquired along with two 1D cross polarization (CP) spectra. The two CP spectra used a short contact time (30 μs) to observe only the protonated carbons signal and a longer contact time (5−20 ms) to observe all of the carbons.[21,22] An additional dipolar dephasing spectrum[23] (dephasing time of 40 μs) produced a distorted line shape due only to the nonprotonated carbons. At room temperature a recycle time of 2 s was used; at 100 K this time had to be increased to 10−20 s. At low temperature (approximately 100 K), only the 1D spectra were recorded as the need for longer recycle times did not allow the acquisition of a 2D MAT of sufficient signal to noise at this temperature. All spectra were taken under slow spinning conditions (approximately 20 Hz) to alleviate a large magic angle hole in the room temperature static spectra of both samples. Data were transferred to a VAX computer for processing and spectral line shape fitting.[24]

Quantum Mechanical Calculations

HF geometry optimizations and calculations of the shielding tensor were performed with the Gaussian 94 computer program[25] on corannulene, coronene, and circumcoronene ($C_{54}H_{18}$). All chemical shift calculations employ the GIAO[26] (gauge invariant atomic orbitals) method and D95** basis sets.[27] For coronene and corannulene, calculations of the shielding tensor were completed on both the X-ray geometries and geometries optimized at the same basis set. The calculated shieldings (σ_c) were converted to the TMS chemical shift scale (δ_c) by $\delta_c = -\sigma_c + 195$, where 195 ppm is the TMS shielding value. This value is the calculated shielding value for methane using the same basis set (202 ppm) minus the 7 ppm difference between these shieldings reported in the literature.[28]

Results and Discussion

In both coronene and corannulene there are three magnetically distinct types of carbons: the inner bridgehead or hub carbons, the outer bridgehead or rim carbons, and the protonated carbons. The $C_{hub}-C_{rim}$ bond defines the "radial" spoke. X-ray structures have been obtained at room temperature for coronene[29] and at both room temperature and −70 °C for corannulene.[30] In both X-ray structures there are slight differences between the various bond lengths and angles which one would expect to be equivalent by the symmetry of an isolated molecule; in corannulene there also exists two distinct molecules per unit cell. In coronene the X-ray structure indicates that the molecule is not exactly planar, with the outermost protonated carbons deviating from planarity by about 2°−4°.

Figure 2 shows the isotropic projection and the 1D slices obtained from the room temperature MAT experiment on corannulene. Similar data was obtained on coronene. At room temperature the existence of the MAT data allows for certainty in the matching between the perpendicular and the parallel components of a specific carbon. The measured principal values are given in Table 1. In the case of coronene, the principal values obtained at room temperature are consistent with the results of both earlier experiments.[10,11]

Unfortunately, the longer recycle times at low temperature prohibits the acquisition of low-temperature 2D MAT spectra of sufficient signal to noise on these compounds; therefore only a tentative pairing of the shift components of the two bridgehead carbons at low temperature is possible. Instead, various 1D spectra (long contact time, short contact time and dipolar

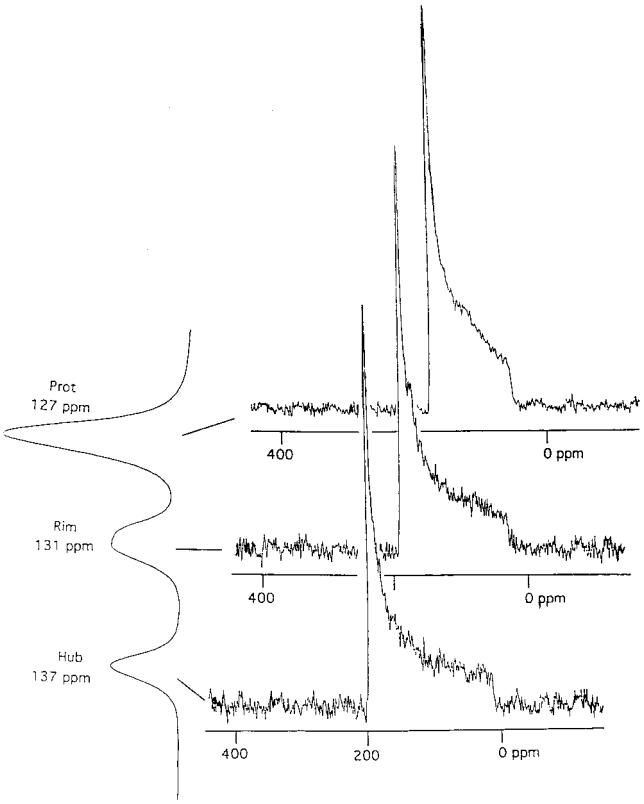

Figure 2. Isotropic projection and the slices taken from the room temperature 2D MAT spectrum of corannulene.

TABLE 1: Experimental Principal Values of the Shift Tensor of Corannulene and Coronene

	room temperature					low temperature			
carbon	δ_{11}	δ_{22}	δ_{33}	δ_{iso}	δ_{mas}	δ_{11}	δ_{22}	δ_{33}	δ_{iso}
				Corannulene					
hub	195	195	15	135	136	224	177	6	136
rim	181	181	27	130	131	214	189	−10	131
protonated	165	165	50	127	127	215	145	17	126
				Coronene					
hub	193	193	−23	121	120	199	199	−38	120
rim	193	193	−15	124	126	204	193	−28	123
protonated	177	177	14	123	123.5	225	137	7	123

dephased) of both compounds were obtained at 100 K; these spectra for corannulene are shown in Figure 3, while those of coronene are given in Figure 4. The short contact time CP experiments on both samples (Figures 3c and 4c) show the expected distortion from an idealized line shape; however, this distortion does not interfere with the ability to accurately pick the breakpoints of the line shape. The simulation of the long contact time line shapes (Figures 3a and 4a) results from the composite of the principal values of the protonated carbons obtained from the short contact time spectra and those of the nonprotonated carbons obtained from the dipolar dephasing spectra. The agreement between the experimental and simulated line shape is considered to be excellent. The principal values at low temperature are also reported in Table 1. The pairing given in the table is that which gives the best fit of the spectrum along with a favorable agreement between the average of the three components and the MAS value. The uncertainties in the experimentally measured values are estimated to be ±3 ppm.

Both compounds exhibit motion at room temperature that averages primarily δ_{11} and δ_{22}, as expected if the molecular motion is rotation about either the five- or sixfold symmetry axis. However, the δ_{33} components also change between room

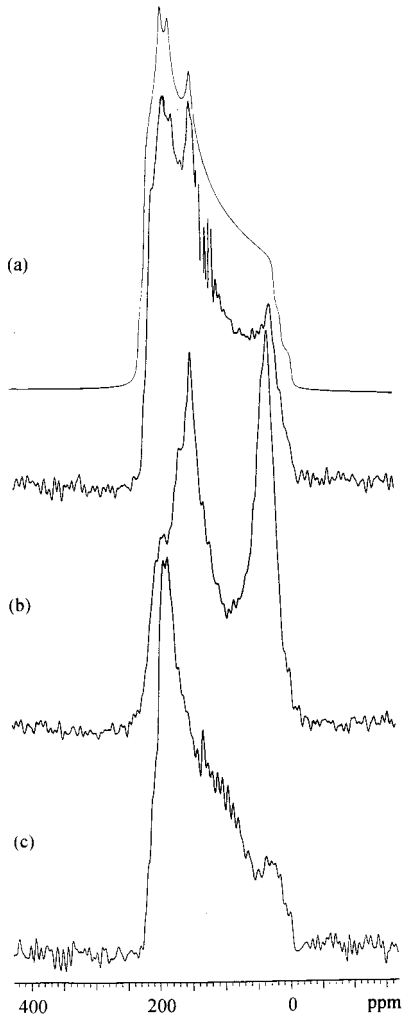

Figure 3. Experimental 1D spectra of corannulene taken at 100 K with (a) long contact time, (b) short contact time, and (c) dipolar dephasing. The simulated line shape included with the long contact time spectrum uses the principal values obtained from fitting the short contact time and dipolar dephased powder patterns.

and low temperature. This was expected in the case of the nonplanar corannulene but was completely unexpected in the planar coronene. The implications of this change in δ_{33} between the two temperatures will be discussed below. Based on the behavior of the static line shape at other temperatures, it is believed that by 100 K the motion has been stopped.

The calculated principal values, both for the X-ray geometries and for the optimized geometries, are reported in Table 2. Because of the small differences in bond lengths and angles in the X-ray structures, as well as the presence of two unique molecules per unit cell for corannulene, all of the carbons have slightly different calculated shielding components. These differences are reported in Table 2 as an average value and standard deviation for each type of carbon. The lines in the ^{13}C CP/MAS spectrum were approximately 50 Hz, which is typical for aromatic compounds. There are two explanations for not observing corresponding differences in the experimental principal values and isotropic chemical shifts. First, the chemical shift differences could be nonexistent or smaller than suggested by the calculations, and therefore are not observed in the experiment. Second, there exists enough motion to average these inequalities and eliminate any inhomogeneous broadening due to the minor shift differences. In the optimized structures the molecular symmetry is enforced, and therefore all carbons of a given type have equivalent shifts. The shift components

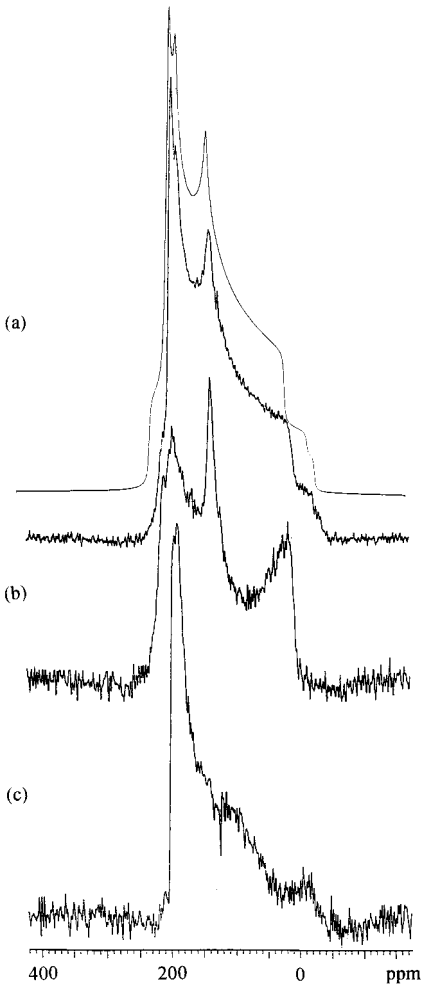

Figure 4. Experimental 1D spectra of coronene taken at 100 K with (a) long contact time, (b) short contact time, and (c) dipolar dephasing. The simulated line shape included with the long contact time spectrum uses the principal values obtained from fitting the short contact time and dipolar dephased powder patterns.

TABLE 2: Calculated Principal Values of the Shift Tensor in Corannulene and Coronene

	X-ray geometry[a,b]				optimized geometry			
carbon	δ_{11}	δ_{22}	δ_{33}	δ_{iso}	δ_{11}	δ_{22}	δ_{33}	δ_{iso}
			Corannulene					
hub	230 ± 9	174 ± 3	0 ± 2	135	228	165	−1	131
	234 ± 6	174 ± 3	2 ± 1	137				
rim	227 ± 16	185 ± 5	-16 ± 2	132	218	176	−13	127
	226 ± 8	183 ± 4	-14 ± 2	132				
protonated	230 ± 18	139 ± 9	5 ± 9	125	226	130	12	123
	230 ± 17	135 ± 5	5 ± 9	123				
			Coronene					
hub	208 ± 7	185 ± 2	-26 ± 1	122	206	179	−23	121
rim	205 ± 11	188 ± 6	-29 ± 4	121	205	189	−25	123
protonated	222 ± 7	123 ± 3	9 ± 3	118	230	123	12	122

[a] The average over all carbons of a given type is reported, as discussed in the text. [b] The first set of values are from the calculation using the geometry at 20 °C and the second set of values are with the geometry at −70 °C.

calculated for the X-ray and the optimized geometries are very similar for coronene. Larger differences, however, are observed between the average of the principal values from the calculation using the experimental geometry and the values obtained with the optimized geometries in corannulene. Unfortunately, there is no trend to indicate which geometry gives the better results. The rms agreement between experiment and theory ranges from

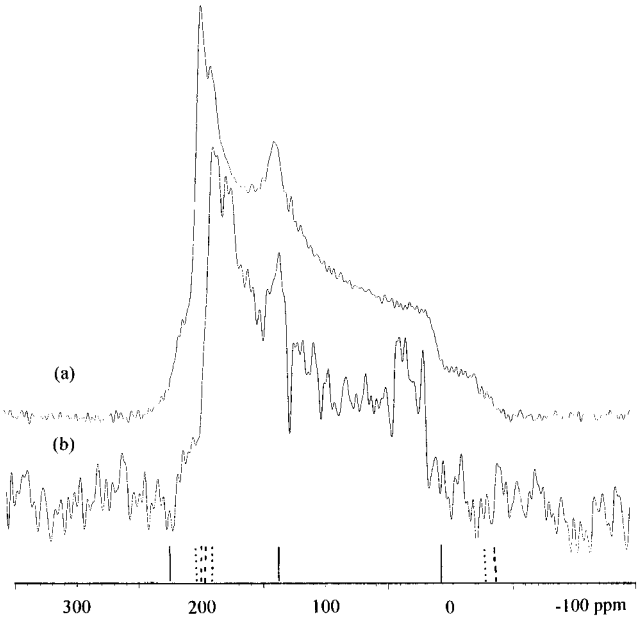

Figure 5. Comparison of spectral pattern obtained for coronene at a temperature of (a) 100 K and (b) 20 K. Lines at the bottom of the figure indicate the position of the tensor components, with solid lines for the protonated carbons, dashed lines for the hub carbons, and dotted lines for the rim carbons.

9 to 11 ppm for the various geometries; this value can be compared to rms values of 4−5 ppm that have been obtained in previous HF level studies of aromatic systems.[1,4,7,8,31] It should be noted that the rms differences are generally lower for single-crystal data, as expected due to lower uncertainties in the experimental quantities.

The most significant difference between theory and experiment is in the δ_{11} and δ_{22} components of the hub carbon in coronene. While, the experimental tensor is axially symmetric, the calculated tensor has a difference of 27 ppm between the two in-plane components. Considering these data alone, it could be concluded that considerable molecular motion is still present at 100 K. However, a comparison between theory and experiment for the other two tensors, especially the outer bridgehead carbon, does not show any indication of the same type of averaging. In addition, a measurement of the static powder pattern of coronene at approximately 20 K is comparable in width to the pattern at 100 K, even though the pattern at the lower temperature is of much lower quality and limits significantly the accuracy of the measured tensor components. This comparison is shown in Figure 5. The lower quality is due to the much smaller sample size that is possible when dealing with the cryogenic apparatus necessary to reach 20 K. Even with the much lower signal to noise, it is evident that the break points in the spectra at the two temperatures generally agree. Therefore, we conclude that the molecular motion has been stopped at 100 K, or at least slowed to a rate below the NMR time scale. Hence, the relatively large discrepancies in the δ_{11} and δ_{22} components of the hub carbon reside in the calculated values. An examination of the crystal structure of coronene shows that the closest intermolecular approach is 2.78 Å (between a carbon of one coronene and a hydrogen on a neighboring molecule). A study of the chemical shielding in naphthalene found intermolecular effects are generally less than 1.5 ppm when the separation between the interacting atoms is 2.4 Å.[32] Therefore, it is believed that the inclusion of intermolecular effects in the calculation on coronene could not lead to the large change necessary to explain these differences. As this discrepancy is observed using

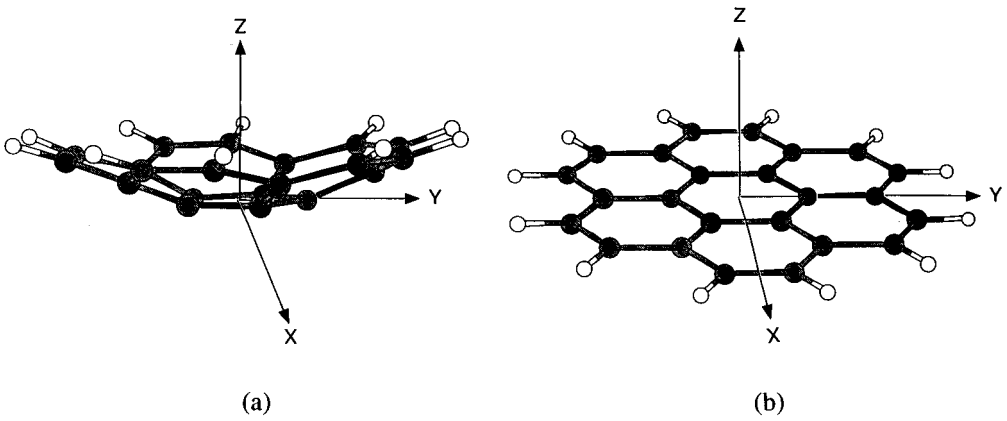

Figure 6. Axis system used in discussion of molecular rotation, as it relates to (a) corannulene and (b) coronene. The *Z* axis is perpendicular to the plane defined by the central ring; *Y* is in this plane and along the $C_{rim}-C_{hub}$ bond (or its projection in the plane of the five-membered ring in the case of corannulene); *X* is in this plane and perpendicular to the $C_{rim}-C_{hub}$ bond (or its projection in the plane of the five-membered ring in the case of corannulene).

TABLE 3: Calculated Principal Values of the Shift Tensor in Circumcoronene

carbon	δ_{11}	δ_{22}	δ_{33}	δ_{iso}	carbon	δ_{11}	δ_{22}	δ_{33}	δ_{iso}
C_a	196	185	−31	117	C_d	224	187	−17	131
C_b	200	186	−28	119	C_e	227	135	34	132
C_c	195	188	−31	118	C_f	261	131	29	140

both X-ray and optimized geometries, we conclude that this difference is an intrinsic deficiency of the HF method used in the calculations.

Shift tensor data for a number of condensed, six-membered ring, aromatic systems exhibit isotropic chemical shifts in the range of 130−140 ppm for bridgehead carbons, with inner bridgehead (e.g., hub) carbons at higher chemical shifts relative to the (e.g., rim) bridgehead carbons. Protonated aromatic carbons generally have isotropic resonances between 120 and 130 ppm. Coronene is an exception to these general trends, with the bridgehead isotropic chemical shifts at 120 and 126 ppm for the hub and rim carbons, respectively. The inner bridgehead carbon of pyrene also has an atypical isotropic chemical shift of 123 ppm.[4] In all three cases, the lower isotropic chemical shift is due to an unusually low δ_{33} component. For example, the δ_{33} component is at −18 ppm in pyrene,[4] whereas the hub and rim bridgehead carbons in coronene have δ_{33} components of −38 and −28 ppm, respectively. A low shift of −30 ppm has also been measured for the δ_{33} component of the bridgehead carbon in a fusinite maceral of coal.[33]

This trend to lower shift values in coronene prompted the completion of a calculation on circumcoronene, shown in Figure 1, to study the effect of even larger ring systems on the value of this component. The results of this calculation are presented in Table 3, using the labeling defined in Figure 1. All of the bridgehead carbons have a δ_{33} component less than 0 ppm, with the innermost bridgehead carbons being the lowest. The calculated values for the bridgehead carbons in circumcoronene are, however, only slightly lower (5−8 ppm) than those calculated for the optimized geometry of coronene, indicating that an asymptotic limit in the δ_{33} component might be expected in large aromatic clusters.

Chemical shift tensor data for five-membered aromatic ring systems are not as widespread. The only compounds with aromatic five-membered rings for which the chemical shift tensors have been measured are C_{60}[14] and fluorene.[4,13] The best comparison that can be made is between the quite similar principal values of C_{60} (220, 186, 25 ppm)[14] and those of the hub carbon of corannulene (224, 177, 7 ppm). The two aromatic carbons attached to the five-membered ring in fluorene (232, 170, 28 ppm for the aromatic carbon adjacent to the CH_2 moiety and 235, 157, 33 ppm for the second one)[4] also show that the δ_{22} component is mainly responsible for the higher isotropic chemical shift. It should be noted that the hub carbons in corannulene do not show the shift to lower isotropic chemical shifts due to very negative δ_{33} components as is observed in coronene. It is interesting that, in contrast to the situation in coronene, possible Kekule structures for the aromatic bonding in corannulene do not involve the central ring in the delocalization of the aromatic π-structure.

Orientation Information

The reference frame used in the following discussion is shown in Figure 6. The five- or sixfold symmetry axis (for corannulene and coronene, respectively), designated the *Z* axis, is the rotation axis for the room temperature motion. The other two axes, *X* and *Y*, are in the plane defined by either the inner bridgehead or hub carbons. The *Y* axis is parallel and the *X* axis perpendicular to the $C_{rim}-C_{hub}$ bond direction for coronene. For corannulene, the *Y* and *X* axes are parallel and perpendicular, respectively, to the projection of the $C_{rim}-C_{hub}$ bond into the plane defined by the five-membered ring of hub carbons.

In previous studies of aromatic systems, both experimental[1−7,31] and theoretical,[34] it has been found that the δ_{33} component is oriented along the p orbitals involved in π-bonding, with the other two components lying in the plane perpendicular to these p orbitals. The δ_{11} component then lies in a direction that tends to be perpendicular to the bond with the highest π-character. The central δ_{22} component is mutually perpendicular to the δ_{11} and δ_{33} components. This rule depends on the extent of conjugation of the π-bonds of adjacent carbons.

Corannulene. Symmetry requires that one component of the chemical shift tensor be perpendicular to the plane of symmetry that contains the $C_{rim}-C_{hub}$ bond (i.e., along the *X* axis) for both of the bridgehead carbons. The component in this direction is expected to be δ_{11} for both the rim and hub carbon, as the $C_{rim}-C_{hub}$ bond has the highest π-character of all the bonds;[34] this assumption is supported by the calculations. The observation that δ_{33} in the low-temperature case is not the same as $\delta_{||}$ in the room temperature case indicates that the direction of δ_{33} does not coincide with the direction of the *Z* axis. In this simplified case, the relationship between the principal values measured for the rotating molecule ($\delta_{\perp}$,$\delta_{||}$) and the static molecule (δ_{11},

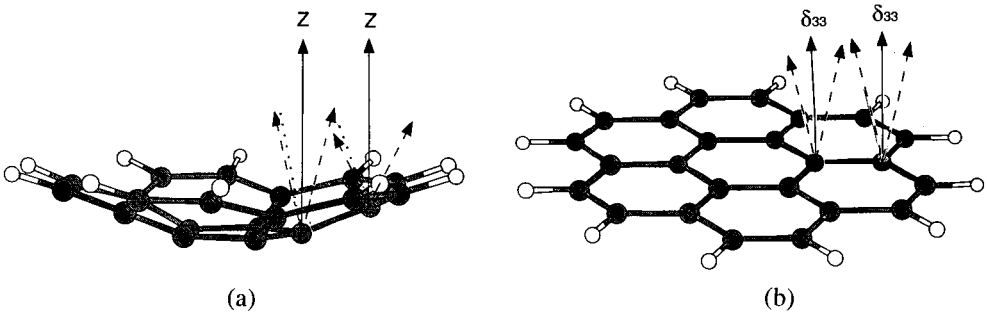

Figure 7. (a) Direction of the δ_{33} component for each of the two bridgehead carbons in corannulene, relative to the *Z* axis (solid arrow). The dashed arrows indicate the two alternative experimental possibilities for each bridgehead, while the dotted lines are the corresponding calculated orientations. (b) Direction of the axis of rotation (dashed arrows), relative to the direction of the δ_{33} component (solid arrow; also the direction of *Z* axis) for the two bridgehead carbons in coronene.

δ_{22}, δ_{33}) can be given as[15]

$$\delta_{||} = (\sin^2 \alpha)\delta_{22} + (\cos^2 \alpha)\delta_{33} \quad (1)$$

$$\delta_{\perp} = {}^1/_2[\delta_{11} + (\cos^2 \alpha)\delta_{22} + (\sin^2 \alpha)\delta_{33}] \quad (2)$$

where α is the angle between the *Z* axis and the direction of the δ_{33} component (or alternately the angle between the *Y* axis and the direction of the δ_{22} component). Using eq 1 results in an angle α of 13° for the hub carbons and 26° for the rim carbons; using eq 2 gives 15° and 27°, respectively. These minor differences in the estimated angles fall within the uncertainties in the measured principal values (±3 ppm). The sign of the angles cannot be experimentally determined, resulting in the two possible orientations shown in Figure 7a with dashed arrows. The calculations of the shielding tensor support this direction, with the angle α being calculated as 10° for the hub carbons and 24° for the rim carbon, in the direction indicated in Figure 7a in dotted lines.

The lack of symmetry planes passing through the protonated carbons prevents an experimental determination of the relative orientation between the PAS and the rotational axis system. However, the general expressions relating the two axis systems can be used, in conjunction with the theoretical principal axis system information, to predict the expected average values:[14]

$$\delta_{\perp} = {}^1/_2(1 - \cos^2\beta \sin^2 \alpha)\delta_{11} + {}^1/_2(1 - \sin^2\beta \sin^2 \alpha)\delta_{22} + {}^1/_2(\sin^2 \alpha)\delta_{33} \quad (3)$$

$$\delta_{||} = (\cos^2\beta \sin^2 \alpha)\delta_{11} + (\sin^2\beta \sin^2 \alpha)\delta_{22} + (\cos^2 \alpha)\delta_{33} \quad (4)$$

where β is the angle between the direction of the δ_{11} component and the C−H bond and α is the angle between the direction of the δ_{33} component and the *Z* axis. Using the theoretically determined values of $\beta = 22°$ and $\alpha = 15°$, the expected principal values due to the rotational averaging of the static experimental principal values are $\delta_{\perp} = 166$ and $\delta_{||} = 44$ ppm, in reasonable agreement with the measured values of $\delta_{\perp} = 165$ and $\delta_{||} = 50$ ppm obtained from the room temperature spectrum.

From Figure 7a, it can be seen that the δ_{33} components of the rim and hub carbons are both nearly perpendicular to the $C_{rim}-C_{hub}$ bond. The angle between the $C_{rim}-C_{hub}$ bond and the δ_{33} component is 82°−84° (theory gives 79°) for the rim carbon and 86°−87° (theory gives 88°) for the hub carbon. This finding is consistent with all previous work on aromatic systems which places the δ_{33} component along the direction of the π-electrons, i.e., perpendicular to the nodal plane of the π-system. Most aromatic systems are planar, and one of the components is required to be perpendicular to the plane by symmetry constraints. In the case of ferrocene,[16] where the π-system is distorted from planarity by the presence of the Fe atom, the δ_{33} component was shown to lie nearly perpendicular to the nodal plane of the π-system. In the case of corannulene, the nonplanar structure leads to the measured orientation of this component. From the X-ray structure, the $C_{rim}-C_{hub}$ bond is found to have an average angle of 22.4° relative to the plane defined by the central five-membered ring. The bonds between the rim and protonated carbons have an average angle of 34.0° from this same plane. These angles provide a fairly good estimate of the angles found for the orientation of the δ_{33} component; i.e., the 11.2° average of the 0° and 22.4° at the hub carbon is in reasonable agreement with the 13° found experimentally, as is the 28.2° average of the 22.4° and 34.0° angles at the rim carbon with the experimental result of 26°. Thus, the π-system would appear to dominate the orientation of this component in corannulene as it does in all other aromatic systems studied.

Coronene. In the case of coronene, an essentially planar molecule, the observation that δ_{33} was not equivalent to $\delta_{||}$ was unexpected. The calculations place δ_{33} perpendicular to the plane (or average plane) defined by the carbons atoms, i.e., along the *Z* axis, for both the rim and hub carbons, as expected. If the motion involved only rotation about this *Z* axis, δ_{33} should be along the rotation direction and the magnitude of the component in the *Z* direction should not change between two spectra; i.e., δ_{33} should be equal to $\delta_{||}$. Using eq 1 to estimate the angle α between the direction of the δ_{33} component and the rotation axis gives 15° for the hub carbon and 14° for the rim carbon. Using eq 2, the angles are calculated to be 13° for both carbons. In addition, the averaging of the protonated carbon tensor, using expressions 3 and 4, is consistent with the angle between the rotation axis and the δ_{33} component being 14°, assuming the calculated angle of 24° between the δ_{11} component and the C−H bond (β). The tensors expected in the case of motional averaging with these angles are calculated to be $\delta_{||} = 175$ ppm and $\delta_{\perp} = 19$ ppm in good agreement with the measured values of 177 and 14 ppm, respectively.

Two possible explanations exist for this consistent difference between δ_{33} and $\delta_{||}$ for the different carbons in coronene. The first possible explanation is that there is a phase change between room temperature and 100 K. Typically, a phase transition can be identified by powder diffraction, differential scanning calorimetry (DSC), or solid-state NMR.[35] The lack of a significant difference between the isotropic chemical shifts between the room temperature and the low-temperature spectra fails to offer NMR support for the presence of a phase change. Therefore,

DSC studies were performed on the coronene sample between room temperature and 120 K (the lower limit of the instrumentation). In this temperature range, there was no indication of any phase transitions. However, there was a small feature at about 225 K that has been previously reported[36] that may reflect a very small enthalpy and entropy change. It is unlikely that this feature could be due to a significant structural transition.

In the absence of a phase transition between the two temperatures, this result could indicate that the motion is not restricted to only in-plane rotation. Such molecular motion involving an out-of-plane component would allow for the mixing of the out-of-plane δ_{33} component with the two in-plane components, e.g., a rotation about the *Z* axis coupled with a precession wobble. This situation is indicated in Figure 7b, with the *Z* axis and therefore the direction of the δ_{33} component designated by solid arrows, and the precession wobble indicated by dashed arrows. Unfortunately, the NMR data are insufficient to confirm the motional details of such a model. The only definitive statement that can be made is that the averaging observed in the experimental ^{13}C powder patterns is inconsistent with a molecule only undergoing in-plane rotation. This observation is, however, not consistent with the earlier ^{1}H moment analysis on this compound,[12] though the measured effects would be within the errors on this measurement.

Conclusions

The principal values of the chemical shift tensor are measured for coronene and corannulene at room temperature and at 100 K. From a comparison of the values obtained from the motionally averaged room temperature spectrum and those obtained from the static low-temperature spectrum, information about the orientation of the principal axis system and the motion of the molecule is obtained. In the case of corannulene, the averaging observed is consistent with the molecular motion being rotation about the fivefold symmetry axis. The angles between the δ_{33} component and the axis of rotation for both of the bridgehead carbons are consistent with the placement of the δ_{33} component nearly along the p orbitals involved in the π-bonding structure. In the case of coronene, however, the results are not consistent with the molecular motion being only rotation about the sixfold symmetry axis. Instead, the experimental results indicate that the overall motion also includes rotation about the sixfold axis along with some type of out-of-plane component (e.g., some kind of wobble) which allows for the mixing of the in-plane δ_{11} and δ_{22} components with the out-of-plane δ_{33} component. Unfortunately, detailed information about the nature of this motion is unobtainable from the present experimental data.

Theoretical calculations of the shielding tensor for coronene, corannulene, and circumcoronene are also presented. While the agreement between experiment and theory is not as good as that obtained in earlier work, it is more than sufficient to aid in the assignments and to provide the information on orientation due to the large anisotropy.

Acknowledgment. This work was funded by Basic Energy Sciences, U.S. Department of Energy, through grant DE-FG03-94ER14452. Computer resources were provided by the Center for High Performance Computing at the University of Utah.

References and Notes

(1) Iuliucci, R. J.; Phung, C. G.; Facelli, J. C.; Grant, D. M. *J. Am. Chem. Soc.* **1998**, *120*, 9305.

(2) Carter, C. M.; Alderman, D. W.; Grant, D. M. *J. Magn. Reson.* **1987**, *73*, 114.

(3) Sherwod, M. H..; Alderman, D. W.; Grant, D. M. *J. Magn. Reson.* **1989**, *84*, 466.

(4) Buntkowsky, G.; Hoffmann, W.; Kupka, T.; Pasterna, G.; Jaworska, M.; Vieth, H.-M. *J. Phys. Chem. A* **1998**, *102*, 5794.

(5) Carter, C. M.; Alderman, D. W.; Facelli, J. C.; Grant, D. M. *J. Am. Chem. Soc.* **1987**, *109*, 2639.

(6) Sherwood, M. H.; Facelli, J. C.; Alderman, D. W.; Grant, D. M. *J. Am. Chem. Soc.* **1991**, *113*, 750.

(7) Iuliucci, R. J.; Facelli, J. C.; Alderman, D. W.; Grant, D. M. *J. Am. Chem. Soc.* **1995**, *117*, 2336.

(8) Iuliucci, R. J.; Phung, C. G.; Facelli, J. C.; Grant, D. M. *J. Am. Chem. Soc.* **1996**, *118*, 4880.

(9) Duncan, T. M. A *Compilation of Chemical Shift Anisotropies*; Farragut Press: Chicago, IL, 1990.

(10) Resing, H. A.; VanderHart, D. L. *Z. Phys. Chem. N.F.* **1987**, *151*, 137.

(11) Hughes, C. D.; Sherwood, M. H.; Alderman, D. W.; Grant, D. M. *J. Magn. Reson. Ser. A* **1993**, *102*, 58.

(12) Fyfe, C. A.; Dunell, B. A.; Ripmeester, J. *Can. J. Chem.* **1971**, *49*, 3332.

(13) Barich, D. H.; Orendt, A. M.; Hu, J. Z.; Pugmire, R. J.; Grant, D. M. Poster 260, 41st Rocky Mountain Conference on Analytical Chemistry, Denver, CO, August 1999.

(14) Yannoni, C. S.; Johnson, R. D.; Meijer, G.; Bethune, D. S.; Salem, J. R. *J. Phys. Chem.* **1991**, *95*, 9.

(15) Mehring, M. *NMR: Basic Principles and Progress*; Springer Verlag: Heidelberg, Germany, 1976; Vol. 12, p 50.

(16) Orendt, A. M.; Facelli, J. C.; Jiang, Y. J.; Grant, D. M. *J. Phys Chem. A* **1998**, *102*, 7692.

(17) Wemmer, D. E.; Pines, A. *J. Am. Chem. Soc*. **1981**, *103*, 34.

(18) Scott, L. T.; Cheng, P.-C.; Hashemi, M. M.; Bratcher, M. S.; Meyer, D. T.; Warren, H. B. *J. Am. Chem. Soc.* **1997**, *119*, 10963.

(19) Jiang, Y. J. Poster MP294, 37th Experimental NMR Conference, Asilomar, CA, March 1996.

(20) Hu, J. Z.; Wang, W.; Liu, F.; Solum, M. S.; Alderman, D. W.; Pugmire, R. J.; Grant, D. M. *J. Magn. Reson. Ser. A* **1995**, *113*, 210.

(21) Alemany, L. B.; Grant, D. M.; Pugmire, R. J.; Alder, T. D.; Zilm, K. W. *J. Am. Chem. Soc*. **1983**, *105*, 2133.

(22) Alemany, L. B.; Grant, D. M.; Pugmire, R. J.; Alder, T. D.; Zilm, K. W. *J. Am. Chem. Soc*. **1983**, *105*, 2142.

(23) Alemany, L. B.; Grant, D. M.; Pugmire, R. J.; Alder, T. D. *J. Am. Chem. Soc*. **1983**, *105*, 6697.

(24) Alderman, D. W.; Solum, M. S.; Grant, D. M. *J. Chem. Phys.* **1986**, *84*, 3717.

(25) *Gaussian 94* (Revision A.1); Frisch, M. J.; Trucks, G. W.; Schlegel, H. B.; Gill, P. M. W.; Johnson, B. G.; Robb, M. A.; Cheeseman, J. R.; Keith, T. A.; Petersson, G. A.; Montgomery, J. A.; Raghavachari, K.; Al-Laham, M. A.; Zakrzewski, V. G.; Ortiz, J. V.; Foresman, J. B.; Cioslowski, J.; Stefanov, B. B.; Nanayakkara, A.; Challacombe, M.; Peng, C. Y.; Ayala, P. Y.; Chen, W.; Wong, M. W.; Andres, J. L.; Replogle, E. S.; Gomperts, R.; Martin, R. L.; Fox, D. J.; Binkley, J. S.; Defrees, D. J.; Baker, J.; Stewart, J. P.; Head-Gordon, M.; Gonzalez, C.; Pople, J. A. Gaussian, Inc.: Pittsburgh, PA, 1995.

(26) Ditchfield, R. *Mol. Phys*. **1974**, *27*, 789.

(27) Dunning, T. H.; Hay, P. J. In *Modern Theoretical Chemistry*; Schaefer, H. F., III, Ed.; Plenum: New York, 1976; p 1.

(28) Jameson, A. K.; Jameson, C. J. *Chem. Phys. Lett.* **1987**, *134*, 461.

(29) Fawcett, J. K.; Trotter, J. *Proc. R. Soc.* **1966**, *A289*, 366.

(30) Hanson, J. C.; Nordman, C. E. *Acta Crystallogr*. **1976**, *B32*, 1147.

(31) Orendt, A. M.; Hu, J. Z.; Jiang, Y. J.; Facelli, J. C.; Wang, W.; Pugmire, R. J.; Ye, C.; Grant, D. M. *J. Phys. Chem. A* **1997**, *101*, 9169.

(32) Facelli, J. C.; Grant, D. M. *Nature* **1993**, *365*, 325.

(33) Sethi, N. K.; Pugmire, R. J.; Facelli, J. C.; Grant, D. M. *Anal. Chem.* **1988**, *60*, 1574.

(34) Facelli, J. C.; Grant, D. M. *Theor. Chim Acta* **1987**, *71*, 277.

(35) Threlfall, T. L. *Analyst* **1995**, *120*, 2435.

(36) Domalski, E. S.; Evans, W. H.; Hearing, E. D. *J. Phys. Chem. Ref. Data* **1984**, *13*, Suppl 1, 236.